

A Discontinuous Enrichment Method (DEM) for Advection-Dominated Fluid Problems

Irina Kalashnikova, Radek Tezaur, Charbel Farhat
Institute for Computational & Mathematical Engineering
Stanford University

Farhat Research Group (FRG) Seminar
Thursday, November 5, 2009



2D Scalar Advection-Diffusion Equation

Scalar Advection-Diffusion Equation

$$\mathcal{L}u = \underbrace{-\kappa \Delta u}_{\text{diffusion}} + \underbrace{\mathbf{a} \cdot \nabla u}_{\text{advection}} = f$$

- Advection velocity:
 $\mathbf{a} = (a_1, a_2)^T = |\mathbf{a}|(\cos \phi, \sin \phi)^T$.
 - $\phi =$ advection direction.
 - $\kappa \equiv 1 =$ diffusivity.
-
- *Why advection-diffusion?*
 - *Why a special finite element method (FEM)?*



2D Scalar Advection-Diffusion Equation

Scalar Advection-Diffusion Equation

$$\mathcal{L}u = \underbrace{-\kappa \Delta u}_{\text{diffusion}} + \underbrace{\mathbf{a} \cdot \nabla u}_{\text{advection}} = f$$

- Advection velocity:
 $\mathbf{a} = (a_1, a_2)^T = |\mathbf{a}|(\cos \phi, \sin \phi)^T$.
- ϕ = advection direction.
- $\kappa \equiv 1$ = diffusivity.

- Describes many transport phenomena in fluid mechanics.
- Usual scalar model for the more challenging Navier-Stokes equations.
- Global Péclet number (L = length scale associated with Ω):

$$Pe = \frac{\text{rate of advection}}{\text{rate of diffusion}} = \frac{L|\mathbf{a}|}{\kappa} = Re \cdot \begin{cases} Pr & \text{(thermal diffusion)} \\ Sc & \text{(mass diffusion)} \end{cases}$$



Advection-Dominated Regime

- Typical applications: flow is advection dominated.

Advection-Dominated
(High Pe) Regime
↓
Sharp gradients in exact solution
↓
Galerkin FEM inadequate:
spurious oscillations (Fig. 1)

- Some classical remedies:
 - Stabilized FEM methods (SUPG, GLS, USFEM): add weighted residual (numerical diffusion) to variational equation.
 - RFB, VMS, PUM: construct conforming spaces that incorporate knowledge of local behavior of solution.

Figure 1: Galerkin Q_1 solution (color) vs. exact solution (black) as $Pe \uparrow$ ($Pe = 10 \rightarrow 150$)



Idea of DEM

- First developed by Farhat *et. al.* in 2000 for the Helmholtz equation.

Idea.

“Enrich” the usual Galerkin polynomial field \mathcal{V}^P by the free-space solutions to the governing homogeneous PDE $\mathcal{L}u = 0$.

$$u^h = u^P + u^E \in \mathcal{V}^P \oplus (\mathcal{V}^E \setminus \mathcal{V}^P)$$

where

$$\mathcal{V}^E = \text{span}\{u : \mathcal{L}u = 0\}$$

- Simple 1D Example:

$$\begin{cases} u_x - u_{xx} = 1 + x, & x \in (0, 1) \\ u(0) = 0, u(1) = 1 \end{cases}$$

- *Enrichments:* $u_x^E - u_{xx}^E = 0 \Rightarrow u^E = C_1 + C_2 e^x \Rightarrow \mathcal{V}^E = \text{span}\{1, e^x\}$
- *Galerkin FEM polynomials:* $\mathcal{V}_{\Omega^e=(x_j, x_{j+1})}^P = \text{span}\left\{\frac{x_{j+1}-x}{h}, \frac{x-x_j}{h}\right\}$



More on DEM

- Two variants of DEM: “pure DGM” vs. “true DEM”

	DGM	DEM
\mathcal{V}^h	\mathcal{V}^E	$\mathcal{V}^P \oplus (\mathcal{V}^E \setminus \mathcal{V}^P)$
u^h	u^E	$u^P + u^E$



Enrichment-only “pure DGM”:

Contribution of the standard polynomial field is dropped from the approximation entirely



Genuine or “full” DEM:

Splitting of the approximation into coarse (polynomial) and fine (enrichment) scales.

- Unlike PUM, VMS & RFB: enrichment field in DEM is not required to vanish at element boundaries



More on DEM

- Two variants of DEM: “pure DGM” vs. “true DEM”

	DGM	DEM
\mathcal{V}^h	\mathcal{V}^E	$\mathcal{V}^P \oplus (\mathcal{V}^E \setminus \mathcal{V}^P)$
u^h	u^E	$u^P + u^E$



Enrichment-only “pure DGM”:

Contribution of the standard polynomial field is dropped from the approximation entirely



Genuine or “full” DEM:

Splitting of the approximation into coarse (polynomial) and fine (enrichment) scales.

- Unlike PUM, VMS & RFB: enrichment field in DEM is not required to vanish at element boundaries \Rightarrow DEM is discontinuous by construction!

DEM = DGM with Lagrange Multipliers



What about Inter-Element Continuity?

- Continuity across element boundaries is enforced weakly using Lagrange multipliers $\lambda^h \in \mathcal{W}^h$:

$$\lambda^h \approx \nabla u_e^E \cdot \mathbf{n}^e = -\nabla u_{e'}^E \cdot \mathbf{n}^{e'} \quad \text{on } \Gamma^{e,e'}$$

but making sure we uphold the...

- Discrete Babuška-Brezzi *inf-sup* condition¹:

$$\left\{ \begin{array}{l} \# \text{ Lagrange multiplier} \\ \text{constraint equations} \end{array} \leq \begin{array}{l} \# \text{ enrichment} \\ \text{equations} \end{array} \right\}$$

Rule of thumb to satisfy the Babuška-Brezzi *inf-sup* condition is to limit:

$$n^\lambda = \left\lfloor \frac{n^E}{4} \right\rfloor \equiv \max \left\{ n \in \mathbb{Z} \mid n \leq \frac{n^E}{4} \right\}$$

$$n^\lambda = \# \text{ Lagrange multipliers per edge,}$$

$$n^E = \# \text{ enrichment functions}$$

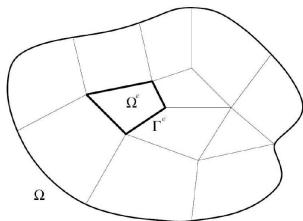
¹Necessary condition for generating a non-singular global discrete problem. 



Hybrid Variational Formulation of DEM

- Strong form:

$$(S) : \begin{cases} \text{Find } u \in H^1(\Omega) \text{ such that} \\ -\Delta u + \mathbf{a} \cdot \nabla u = f, & \text{in } \Omega \\ u = g, & \text{on } \Gamma = \partial\Omega \\ u_e - u_{e'} = 0 & \text{on } \Gamma^{\text{int}} \end{cases}$$



- Weak hybrid variational form:

$$(W) : \begin{cases} \text{Find } (u, \lambda) \in \mathcal{V} \times \mathcal{W} \text{ such that:} \\ a(v, u) + b(\lambda, v) = r(v) \\ b(\mu, u) = -r_d(\mu) \\ \text{holds } \forall v \in \mathcal{V}, \forall \mu \in \mathcal{W}. \end{cases}$$

Figure 2: Discretization of domain into elements Ω^e

where

$$a(v, u) = (\nabla v + v\mathbf{a}, \nabla u)_{\tilde{\Omega}}$$

$$b(\lambda, v) = \sum_e \sum_{e' < e} \int_{\Gamma^{e,e'}} \lambda (v_{e'} - v_e) d\Gamma + \int_{\Gamma} \lambda v d\Gamma$$

Notation:

$$\tilde{\Omega} = \cup_{e=1}^{n_{el}} \Omega^e$$

$$\tilde{\Gamma} = \cup_{e=1}^{n_{el}} \Gamma^e$$

$$\Gamma^{e,e'} = \Gamma^e \cap \Gamma^{e'}$$

$$\Gamma^{\text{int}} = \cup_{e' < e} \cup_{e=1}^{n_{el}} \{\Gamma^e \cap \Gamma^{e'}\}$$

Implementation & Computational Complexity

- Element matrix problem (uncondensed):

$$\begin{pmatrix} \mathbf{k}^{PP} & \mathbf{k}^{PE} & \mathbf{k}^{PC} \\ \mathbf{k}^{EP} & \mathbf{k}^{EE} & \mathbf{k}^{EC} \\ \mathbf{k}^{CP} & \mathbf{k}^{CE} & \mathbf{0} \end{pmatrix} \begin{pmatrix} \mathbf{u}^P \\ \mathbf{u}^E \\ \lambda^h \end{pmatrix} = \begin{pmatrix} \mathbf{r}^P \\ \mathbf{r}^E \\ \mathbf{r}^C \end{pmatrix}$$



Implementation & Computational Complexity

- Element matrix problem (uncondensed):

$$\begin{pmatrix} \mathbf{k}^{PP} & \mathbf{k}^{PE} & \mathbf{k}^{PC} \\ \mathbf{k}^{EP} & \mathbf{k}^{EE} & \mathbf{k}^{EC} \\ \mathbf{k}^{CP} & \mathbf{k}^{CE} & \mathbf{0} \end{pmatrix} \begin{pmatrix} \mathbf{u}^P \\ \mathbf{u}^E \\ \lambda^h \end{pmatrix} = \begin{pmatrix} \mathbf{r}^P \\ \mathbf{r}^E \\ \mathbf{r}^C \end{pmatrix}$$

Due to the discontinuous nature of \mathcal{V}^E , u^E can be eliminated at the element level by a static condensation.



Implementation & Computational Complexity

- Element matrix problem (uncondensed):

$$\begin{pmatrix} \mathbf{k}^{PP} & \mathbf{k}^{PE} & \mathbf{k}^{PC} \\ \mathbf{k}^{EP} & \mathbf{k}^{EE} & \mathbf{k}^{EC} \\ \mathbf{k}^{CP} & \mathbf{k}^{CE} & \mathbf{0} \end{pmatrix} \begin{pmatrix} \mathbf{u}^P \\ \mathbf{u}^E \\ \lambda^h \end{pmatrix} = \begin{pmatrix} \mathbf{r}^P \\ \mathbf{r}^E \\ \mathbf{r}^C \end{pmatrix}$$

Due to the discontinuous nature of \mathcal{V}^E , u^E can be eliminated at the element level by a static condensation.

- Statically-condensed True DEM Element:

$$\begin{pmatrix} \tilde{\mathbf{k}}^{PP} & \tilde{\mathbf{k}}^{PC} \\ \tilde{\mathbf{k}}^{CP} & \tilde{\mathbf{k}}^{CC} \end{pmatrix} \begin{pmatrix} \mathbf{u}^P \\ \lambda^h \end{pmatrix} = \begin{pmatrix} \tilde{\mathbf{r}}^P \\ \tilde{\mathbf{r}}^C \end{pmatrix}$$

- Statically-condensed Pure DGM Element:

$$-\mathbf{k}^{CE}(\mathbf{k}^{EE})^{-1}\mathbf{k}^{EC}\lambda^h = \mathbf{r}^C - \mathbf{k}^{CE}(\mathbf{k}^{EE})^{-1}\mathbf{r}^E,$$



Implementation & Computational Complexity

- Element matrix problem (uncondensed):

$$\begin{pmatrix} \mathbf{k}^{PP} & \mathbf{k}^{PE} & \mathbf{k}^{PC} \\ \mathbf{k}^{EP} & \mathbf{k}^{EE} & \mathbf{k}^{EC} \\ \mathbf{k}^{CP} & \mathbf{k}^{CE} & \mathbf{0} \end{pmatrix} \begin{pmatrix} \mathbf{u}^P \\ \mathbf{u}^E \\ \lambda^h \end{pmatrix} = \begin{pmatrix} \mathbf{r}^P \\ \mathbf{r}^E \\ \mathbf{r}^C \end{pmatrix}$$

Computational complexity depends on $\dim\{\mathcal{W}^h\}$,
not $\dim\{\mathcal{V}^E\}$

Due to the discontinuous nature of \mathcal{V}^E , u^E can be eliminated at the element level by a static condensation.



- Statically-condensed True DEM Element:

$$\begin{pmatrix} \tilde{\mathbf{k}}^{PP} & \tilde{\mathbf{k}}^{PC} \\ \tilde{\mathbf{k}}^{CP} & \tilde{\mathbf{k}}^{CC} \end{pmatrix} \begin{pmatrix} \mathbf{u}^P \\ \lambda^h \end{pmatrix} = \begin{pmatrix} \tilde{\mathbf{r}}^P \\ \tilde{\mathbf{r}}^C \end{pmatrix}$$

- Statically-condensed Pure DGM Element:

$$-\mathbf{k}^{CE}(\mathbf{k}^{EE})^{-1}\mathbf{k}^{EC}\lambda^h = \mathbf{r}^C - \mathbf{k}^{CE}(\mathbf{k}^{EE})^{-1}\mathbf{r}^E,$$



Angle-Parametrized Enrichment Functions for 2D Advection-Diffusion

- Derived by solving $\mathcal{L}u^E = \mathbf{a} \cdot \nabla u^E - \Delta u^E = 0$ analytically (e.g., separation of variables).

$$u^E(\mathbf{x}; \theta_i) = e^{Pe \left(\frac{\cos \phi + \cos \theta_i}{2} \right) (x - x_{r,i})} e^{Pe \left(\frac{\sin \phi + \sin \theta_i}{2} \right) (y - y_{r,i})} \quad (1)$$

$\Theta^u \equiv \{\theta_i\}_{i=1}^{n^E} \in [0, 2\pi) =$ set of angles specifying \mathcal{V}^E

$(x_{r,i}, y_{r,i}) =$ reference point for u_i^E

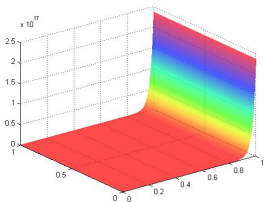
$\phi \in [0, 2\pi) =$ advection direction

The parametrization with respect to θ_i in (2) is non-trivial!

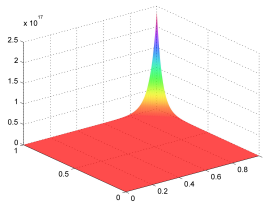
- Enrichment functions are now specified by a set of “flow directions”.
- Without this parametrization, systematic element design would not be possible!



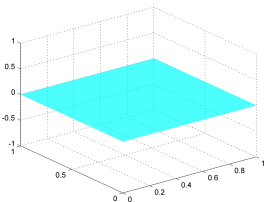
Plots of Enrichment Functions for Some Angles $\theta_i \in [0, 2\pi)$



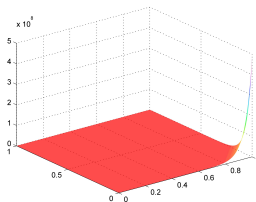
$$\theta_i = 0$$



$$\theta_i = \frac{\pi}{2}$$



$$\theta_i = \pi$$



$$\theta_i = \frac{3\pi}{2}$$

Figure 3: Plots of enrichment function $u^E(\mathbf{x}; \theta_i)$ for several values of θ_i ($\phi = 0$)



What about the Lagrange Multiplier Approximations?

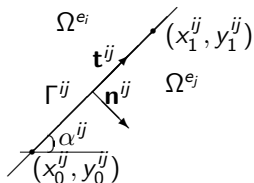


Figure 4: Straight edge Γ^{ij} oriented at angle $\alpha^{ij} \in [0, 2\pi)$

- Trivial to compute given exponential enrichments:

$$\begin{aligned} \lambda^h(s)|_{\Gamma^{ij}} &\approx \nabla u^E \cdot \mathbf{n}|_{\Gamma_{e,e'}} \\ &= e^{\left\{ \frac{|a|}{2} [\cos(\phi - \alpha^{ij}) + \cos(\theta_k - \alpha^{ij})] (s - s_r^{ij}) \right\}} \end{aligned}$$

- Non-trivial to satisfy *inf-sup* condition: the set Θ^u that defines \mathcal{V}^E typically leads to too many Lagrange multiplier dofs!



What about the Lagrange Multiplier Approximations?

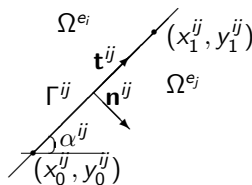


Figure 4: Straight edge Γ^{ij} oriented at angle $\alpha^{ij} \in [0, 2\pi)$

- Trivial to compute given exponential enrichments:

$$\begin{aligned} \lambda^h(s)|_{\Gamma^{ij}} &\approx \nabla u^E \cdot \mathbf{n}|_{\Gamma_{e,e'}} \\ &= e^{\left\{ \frac{|a|}{2} [\cos(\phi - \alpha^{ij}) + \cos(\theta_k^\lambda - \alpha^{ij})](s - s_r^{ij}) \right\}} \end{aligned}$$

- Non-trivial to satisfy *inf-sup* condition: the set Θ^u that defines \mathcal{V}^E typically leads to too many Lagrange multiplier dofs!



- Select $\Theta^\lambda \not\subset \Theta^u$ (set to define \mathcal{W}^h) independently of Θ^u , with $\text{card}\{\Theta^\lambda\} \equiv n^\lambda = \left\lfloor \frac{n^E}{4} \right\rfloor$.

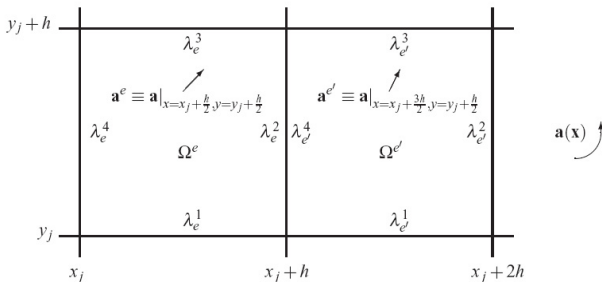
$$\Theta^\lambda = \{\theta_k^\lambda\}_{k=1}^{n^\lambda} = \text{set of angles that specifies the Lagrange multipliers}$$



Extension to the Variable-Coefficient Advection-Diffusion Equation

- $\mathbf{a}(\mathbf{x}) \approx \mathbf{a}^e = \text{constant}$ inside each element Ω^e as $h \rightarrow 0$:

$$\{\mathbf{a}(\mathbf{x}) \cdot \nabla u - \kappa \Delta u = f(\mathbf{x}) \text{ in } \Omega\} \approx \cup_e^{n_{el}} \{\mathbf{a}^e \cdot \nabla u - \kappa \Delta u = f(\mathbf{x}) \text{ in } \Omega^e\}$$



- Define \mathcal{V}^E *within each element* as the free-space solutions to the homogeneous PDE, with locally-frozen coefficients.

$$u_e^E(\mathbf{x}; \theta_i^e) = e^{\frac{|\mathbf{a}^e|}{2\kappa} (\cos \phi^e + \cos \theta_i^e)(x - x_{r,i}^e)} e^{\frac{|\mathbf{a}^e|}{2\kappa} (\sin \phi^e + \sin \theta_i^e)(y - y_{r,i}^e)} \in \mathcal{V}_e^E, \quad \mathcal{V}^E = \cup_e \mathcal{V}_e^E$$

$$\mathcal{W}_{e,e'}^h \equiv \text{span} \left\{ \nabla c_{e,e'}^E(\mathbf{x}; \theta_i^{\lambda_{e,e'}}) |_{\Gamma_{e,e'}} \cdot \mathbf{n}^{e,e'} : \text{card}\{\Theta_{e,e'}^\lambda\} = \left\lfloor \frac{n^E}{4} \right\rfloor \right\}$$



Mesh Independent Element Design Procedure

Algorithm 1. “Build your own DEM element”

Fix $n^E \in \mathbb{N}$ (the desired number of angles defining \mathcal{V}^E).

Select a set of n^E distinct angles $\{\theta_k\}_{k=1}^{n^E}$ between $[0, 2\pi)$.

Let $\Theta^u = \phi + \{\theta_i\}_{i=1}^{n^E}$.

Define the enrichment functions by:

$$u^E(\mathbf{x}; \Theta^u) = e^{\frac{Pe}{2}(\cos \phi + \cos \Theta^u)(x - x_{r,i})} e^{\frac{Pe}{2}(\sin \phi + \sin \Theta^u)(y - y_{r,i})}$$

Let $n^\lambda = \left\lfloor \frac{n^E}{4} \right\rfloor$.

Choose a set of n^λ distinct angles $\{\beta_k^\lambda\}_{k=1}^{n^\lambda}$ between $[0, \pi)$.

for each edge $\Gamma^{ij} \in \Gamma^{\text{int}}$ having slope α^{ij}

Define the Lagrange multipliers approximations on $\Gamma^{e,e'}$ by:

$$\lambda^h(s)|_{\Gamma^{ij}} = e^{\frac{|a|}{2}[\cos(\phi - \alpha^{ij}) + \cos \beta_k^\lambda]}(s - s_{r,k})$$

end for



Some DGM/DEM Elements

Notation

DGM Element: $Q - n^E - n^\lambda$ DEM Element: $Q - n^E - n^{\lambda+} \equiv [Q - n^E - n^\lambda] \cup [Q_1]$

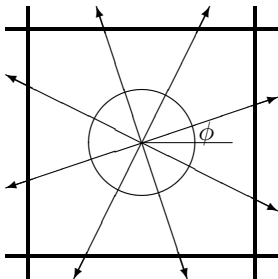
'Q': Quadrilateral

 n^E : Number of Enrichment Functions n^λ : Number of Lagrange Multipliers per Edge Q_1 : Galerkin Bilinear Quadrilateral Element

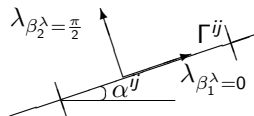
Name	n^E	Θ^u	n^λ	Θ^λ
$Q - 4 - 1$	4	$\phi + \left\{ \frac{m\pi}{2} : m = 0, \dots, 3 \right\}$	1	ϕ
$Q - 8 - 2$	8	$\phi + \left\{ \frac{m\pi}{4} : m = 0, \dots, 7 \right\}$	2	$\alpha^{ij} + \left\{ 0, \frac{\pi}{2} \right\}$
$Q - 12 - 3$	12	$\phi + \left\{ \frac{m\pi}{6} : m = 0, \dots, 11 \right\}$	3	$\alpha^{ij} + \left\{ \frac{\pi}{4}, \frac{\pi}{2}, \frac{3\pi}{4} \right\}$
$Q - 16 - 4$	16	$\phi + \left\{ \frac{m\pi}{8} : m = 0, \dots, 15 \right\}$	4	$\alpha^{ij} + \left\{ 0, \frac{\pi}{4}, \frac{\pi}{2}, \frac{3\pi}{4} \right\}$
$Q - 5 - 1^+$	5	$\phi + \left\{ \frac{2m\pi}{5} : m = 0, \dots, 4 \right\}$	1	$\phi - \pi$
$Q - 9 - 2^+$	9	$\phi + \left\{ \frac{2m\pi}{9} : m = 0, \dots, 8 \right\}$	2	$\alpha^{ij} + \left\{ 0, \frac{\pi}{2} \right\}$
$Q - 13 - 3^+$	13	$\phi + \left\{ \frac{2m\pi}{13} : m = 0, \dots, 12 \right\}$	3	$\alpha^{ij} + \left\{ \frac{\pi}{4}, \frac{\pi}{2}, \frac{3\pi}{4} \right\}$
$Q - 17 - 4^+$	17	$\phi + \left\{ \frac{2m\pi}{17} : m = 0, \dots, 16 \right\}$	4	$\alpha^{ij} + \left\{ 0, \frac{\pi}{4}, \frac{\pi}{2}, \frac{3\pi}{4} \right\}$



Illustration of the Θ^u and Θ^λ for the DGM $Q - 8 - 2$ Element



(a) Enrichment basis



(b) Lagrange multiplier dofs

Figure 5: Illustration of the sets Θ^u and Θ^λ that define the $Q - 8 - 2$ element



Computational Complexity

Table 1: Computational complexities of some DGM, DEM and Galerkin elements.

Element	Asymptotic # of dofs	Stencil width for uniform $n \times n$ mesh
Q_1	n_{el}	9
Q_2	$3n_{el}$	21
Q_3	$5n_{el}$	33
Q_4	$7n_{el}$	45
$Q - 4 - 1$	$2n_{el}$	7
$Q - 8 - 2$	$4n_{el}$	14
$Q - 12 - 3$	$6n_{el}$	21
$Q - 16 - 4$	$8n_{el}$	28
$Q - 5 - 1^+$	$3n_{el}$	21
$Q - 9 - 2^+$	$5n_{el}$	33
$Q - 13 - 3^+$	$7n_{el}$	45
$Q - 17 - 4^+$	$9n_{el}$	57



Homogeneous Boundary Layer Problem

- $\Omega = (0, 1) \times (0, 1)$, $f = 0$.
- Homogeneous problem \Rightarrow pure DGM elements sufficient.
- $\mathbf{a} = Pe \begin{pmatrix} \cos \phi & \sin \phi \end{pmatrix}$.
- Dirichlet boundary conditions are specified on Γ such that the exact solution to the BVP is given by

$$u_{\text{ex}}(\mathbf{x}; \phi, \psi) = \frac{e^{\frac{Pe}{2} \{[\cos \phi + \cos \psi](x-1) + [\sin \phi + \sin \psi](y-1)\}} - 1}{e^{-\frac{Pe}{2} [\cos \phi + \cos \psi + \sin \phi + \sin \psi]} - 1}$$

- $\psi \in [0, 2\pi)$: some flow direction (not necessarily aligned with ϕ).
- Solution exhibits a sharp exponential boundary layer in the advection direction ϕ , whose gradient is a function of the Péclet number.

Figure 6: $\phi = \psi = 0$

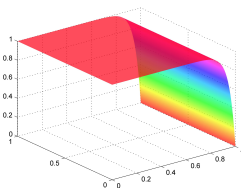
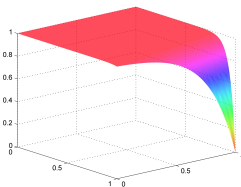


Figure 7: $\phi = \pi/7, \psi = 0$



Flow Aligned with Advection Direction ($\phi = \psi$)

- $u_{ex} \in \mathcal{V}^E$ for *all* DGM elements, for all advection directions ϕ here.



Flow Aligned with Advection Direction ($\phi = \psi$)

- $u_{ex} \in \mathcal{V}^E$ for *all* DGM elements, for all advection directions ϕ here.
- Therefore one would expect these elements to capture the exact solution to machine precision



Flow Aligned with Advection Direction ($\phi = \psi$)

- $u_{ex} \in \mathcal{V}^E$ for all DGM elements, for all advection directions ϕ here.
- Therefore one would expect these elements to capture the exact solution to machine precision – *but only provided* $\nabla u_{ex} \cdot \mathbf{n} \in \mathcal{W}^h$.

Table 2: Relative $L^2(\Omega)$ errors, ≈ 400 dofs, $Pe = 10^3$, uniform mesh: Galerkin vs. DGM elts.

ϕ/π	Q_1	$Q - 4 - 1$	Q_2	$Q - 8 - 2$
0	5.77×10^{-1}	3.43×10^{-14}	4.33×10^{-1}	2.22×10^{-10}
1/6	2.53×10^{-2}	1.24×10^{-15}	1.49×10^{-2}	8.38×10^{-4}
1/4	2.62×10^{-2}	3.19×10^{-14}	1.53×10^{-2}	5.62×10^{-6}
ϕ/π	Q_3	$Q - 12 - 3$	Q_4	$Q - 16 - 4$
0	3.68×10^{-1}	5.78×10^{-13}	2.44×10^{-1}	9.75×10^{-10}
1/6	1.21×10^{-2}	5.50×10^{-6}	9.47×10^{-3}	3.31×10^{-6}
1/4	1.24×10^{-2}	4.36×10^{-14}	9.81×10^{-3}	1.27×10^{-12}



Flow *not* Aligned with Advection Direction ($\phi \neq \psi$)

- Fix $\phi = \pi/7$, vary ψ .



Flow *not* Aligned with Advection Direction ($\phi \neq \psi$)

- Fix $\phi = \pi/7$, vary ψ .
- Can show that $u_{\text{ex}} \notin \mathcal{V}^E$ for any DGM elements and advection directions tested here.

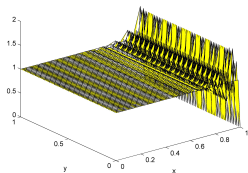
Table 3: Relative $L^2(\Omega)$ errors, ≈ 1600 dofs, unstructured mesh, $\phi = \pi/7$, $Pe = 10^3$: Galerkin vs. DGM elts.

ψ/π	Q_1	$Q - 4 - 1$	Q_2	$Q - 8 - 2$
0	1.45×10^{-2}	1.65×10^{-3}	5.92×10^{-3}	1.79×10^{-3}
1/4	1.52×10^{-2}	9.38×10^{-4}	6.06×10^{-3}	2.54×10^{-4}
1/2	1.51×10^{-2}	9.23×10^{-4}	5.97×10^{-3}	2.12×10^{-4}
ψ/π	Q_3	$Q - 12 - 3$	Q_4	$Q - 16 - 4$
0	4.34×10^{-3}	1.10×10^{-4}	3.23×10^{-3}	2.30×10^{-5}
1/4	4.46×10^{-3}	1.23×10^{-5}	3.29×10^{-3}	8.82×10^{-7}
1/2	4.36×10^{-3}	1.11×10^{-5}	3.18×10^{-3}	1.59×10^{-6}

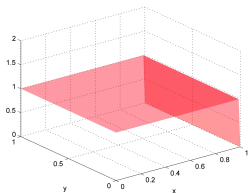


Solution Plots

Figure 8: $\phi = \psi = 0$, $Pe = 10^3$, ≈ 1600 dofs

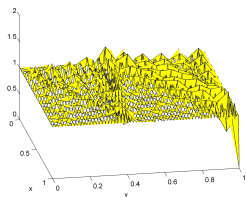


Q_3

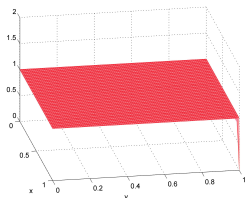


$Q-12-3$

Figure 9: $\phi = \pi/7$, $\psi = 0$, $Pe = 10^5$, ≈ 1600 dofs



Q_3



$Q-12-3$



Convergence Analysis

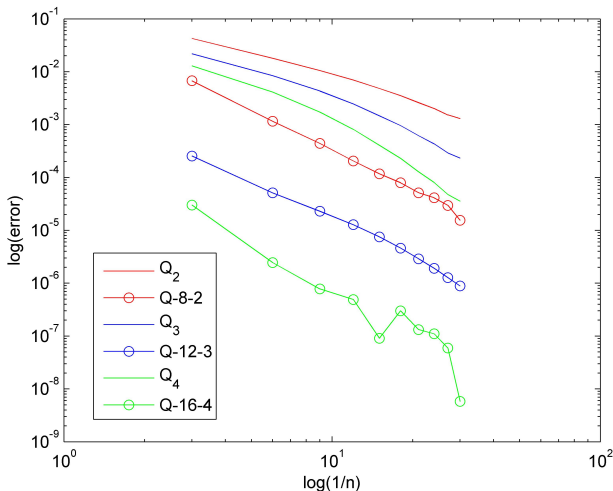
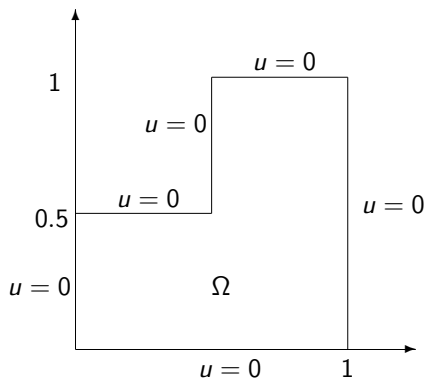


Figure 10: Convergence Rates ($\phi = \pi/7, \psi = 0, Pe = 10^2$, unstructured mesh)



Double Ramp Problem on an L -Shaped Domain

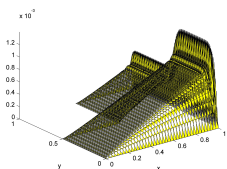


- Homogeneous Dirichlet boundary conditions are prescribed on all six sides of L -shaped domain Ω
- Advection direction: $\phi = 0$
- Source: $f = 1$
- Strong outflow boundary layer along the line $x = 1$
- Two crosswind boundary layers along $y = 0$ and $y = 1$
- A crosswind internal layer along $y = 0.5$

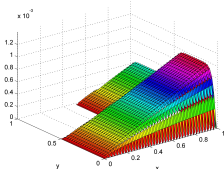


Solutions Plots: Galerkin vs. DGM vs. DEM Elements

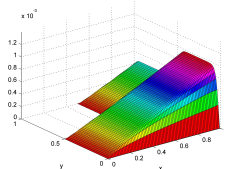
Figure 11: L -shaped double ramp problem solutions: $Pe = 10^3$, 1200 elts.



Q_3



$Q - 12 - 3$



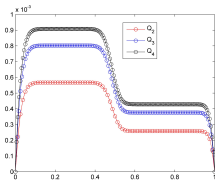
$Q - 13 - 3^+$

- No oscillations can be seen in the computed DGM and DEM solutions.
- Would expect: DEM elements to outperform DGM elements for this *inhomogeneous* problem.
- In fact: DGM elements experience some difficulty along the $y = 0.5$ line, the location of the crosswind internal layer.

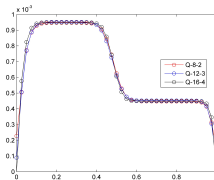


Cross Sectional Solution Plots

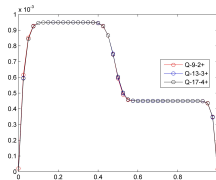
Figure 12: Solution along the line $x = 0.9$ with 1200 elts.



Galerkin

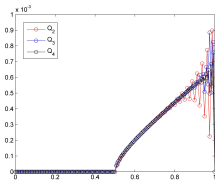


DGM

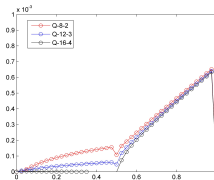


DEM

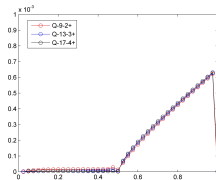
Figure 13: Solution along the line $y = 0.5$ with 1200 elts.



Galerkin



DGM



DEM



Relative Errors

Table 4: $L^2(\Omega)$ errors relative to a reference solution*: uniform mesh, $Pe = 10^3$

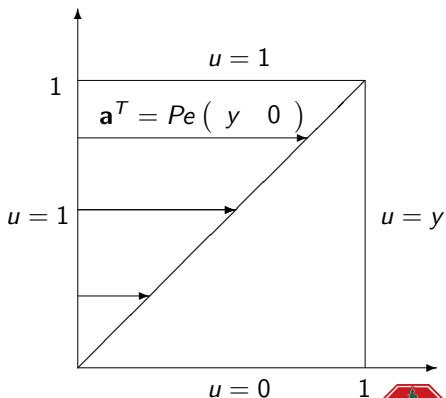
# elements	Q_2	$Q - 8 - 2$	$Q - 9 - 2^+$
300	2.72×10^{-1}	1.19×10^{-1}	4.11×10^{-2}
1200	1.23×10^{-1}	6.07×10^{-2}	8.47×10^{-3}
4800	5.26×10^{-2}	2.81×10^{-2}	1.65×10^{-3}
10,800	2.92×10^{-2}	1.54×10^{-2}	7.43×10^{-4}
# elements	Q_3	$Q - 12 - 3$	$Q - 13 - 3^+$
300	1.49×10^{-1}	1.11×10^{-1}	2.80×10^{-2}
1200	6.57×10^{-2}	5.00×10^{-2}	4.71×10^{-3}
4800	2.36×10^{-2}	1.02×10^{-2}	8.24×10^{-4}
10,800	1.08×10^{-2}	4.54×10^{-3}	9.75×10^{-5}
# elements	Q_4	$Q - 16 - 4$	$Q - 17 - 4^+$
300	9.58×10^{-2}	8.32×10^{-2}	2.16×10^{-2}
1200	3.78×10^{-2}	1.33×10^{-2}	2.94×10^{-3}
4800	1.03×10^{-2}	9.17×10^{-3}	1.26×10^{-4}
10,800	3.70×10^{-3}	4.92×10^{-4}	2.12×10^{-5}

- * Since an analytical solution to this problem is not available, in computing the relative error, we use in place of the exact solution a reference solution, computed using a Galerkin Q_6 polynomial element on a $43,200 = 3 \cdot (120 \times 120)$ element mesh.

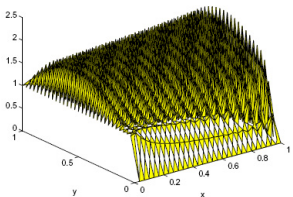
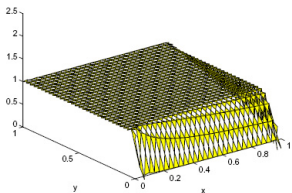
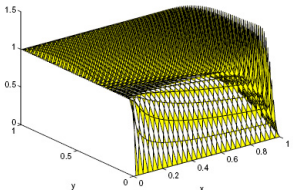
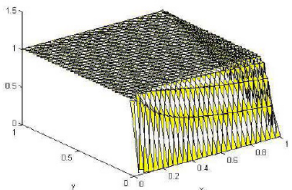


Variable-Coefficient Numerical Example: Thermal Boundary Layer Problem

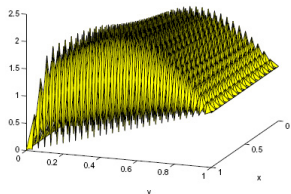
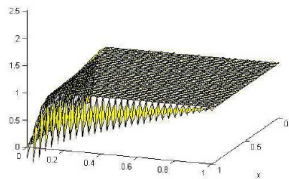
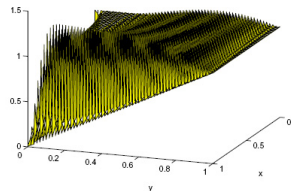
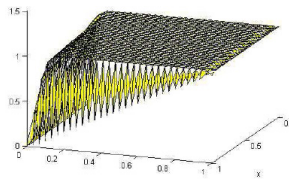
- $\Omega = (0, 1) \times (0, 1)$, $f = 0$.
- $\mathbf{a}^T(\mathbf{x}) = Pe (y \ 0)$
- $u(\mathbf{x})$ represents temperature.
- Model for formation of a pair of thermal boundary layers along the lower and outflow boundaries of a fully developed shear flow between two parallel plates, with the upper plate moving to the right, and the lower plate fixed.
- Main difficulties:
 - Outflow boundary layer at $x = 1$.
 - Parabolic layer along $y = 0$.



Solution Plots for $Pe = 10^4$, uniform 30×30 mesh (Front Views)

 Q_1  $Q-4-1$  Q_2  $Q-8-2$ 

Solution Plots for $Pe = 10^4$, uniform 30×30 mesh (Rear Views)

 Q_1  $Q-4-1$  Q_2  $Q-8-2$ 

Relative Errors

Table 5: $L^2(\Omega)$ errors relative to a reference solution* for $Pe \leq 10^4$

Pe	n	Q_1	$Q - 4 - 1$	Q_2	$Q - 8 - 2$
10^3	15	1.17×10^{-1}	1.83×10^{-2}	5.14×10^{-2}	1.62×10^{-2}
	30	5.79×10^{-2}	8.77×10^{-3}	2.22×10^{-2}	7.64×10^{-3}
10^4	15	2.61×10^0	2.13×10^{-2}	5.93×10^{-1}	2.59×10^{-2}
	30	4.61×10^{-1}	1.09×10^{-2}	1.10×10^{-1}	1.09×10^{-2}

Table 6: $L^2(\Omega)$ errors relative to a reference solution* for $Pe \geq 10^5$ with ≈ 800 dofs

Pe	Q_1	$Q - 4 - 1$
10^5	5.71×10^0	4.56×10^{-2}
10^6	5.40×10^1	1.47×10^{-1}

- * Since an analytical solution to this problem is not available, in computing the relative error, we use in place of the exact solution a reference solution, computed using a Galerkin Q_6 polynomial element on a 60×60 element mesh.



Conclusions & Ongoing Work

- For all test problems, the enriched elements outperform their Galerkin and stabilized Galerkin counterparts of comparable computational complexity by at least one (and sometimes many) orders of magnitude difference on unstructured meshes.
- For $Pe = 10^3$, to achieve a 0.1% level of relative error:
 - $Q - 8 - 2$ and $Q - 9 - 2^+$ elements: reduce the dof requirement of the Q_2 element by a factor between 4.5 and 5.
 - $Q - 12 - 3$ and $Q - 13 - 3^+$ elements: reduce the dof requirement of the Q_3 element by a factor of between 14 and 15.
 - $Q - 16 - 4$ and $Q - 17 - 4^+$ elements: reduce the dof requirement of the Q_4 element by a factor of between 15 and 15.2.
- In a high Péclet regime, DGM and DEM solutions are almost completely oscillation-free, in contrast with the Galerkin solutions.
- Ongoing/future work:
 - DEM for non-linear unsteady problems (e.g., viscous Burgers equation).
 - Projection method-based DEM for incompressible Navier-Stokes.



Questions?

Recent publications (www.stanford.edu/~irinak/pubs.html):

- C. Farhat, I. Kalashnikova, R. Tezaur. A Higher-Order Discontinuous Enrichment Method for the Solution of High Péclet Advection-Diffusion Problems on Unstructured Meshes. *Int. J. Numer. Meth. Engng.* (accepted June 2009).
- I. Kalashnikova, C. Farhat, R. Tezaur. A Discontinuous Enrichment Method for the Solution of Advection-Diffusion Problems in high Péclet Number Regimes. *Fin. El. Anal. Des.* **45** (2009) 238-250.

Thank you!



DEM for the Viscous Burgers Equation ("Hot off the Processor!")

- Non-linear version of advection-diffusion equation = viscous Burgers equation:

$$u_t + uu_x - \kappa u_{xx} = 0$$

- Semi-discrete form of PDE (with Euler scheme) at time n :

$$\frac{u^{n+1} - u^n}{\Delta t} + u^n u_x^{n+1} - \kappa u_{xx}^{n+1} = 0 \quad (2)$$



DEM for the Viscous Burgers Equation (“Hot off the Processor!”)

- Non-linear version of advection-diffusion equation = viscous Burgers equation:

$$u_t + uu_x - \kappa u_{xx} = 0$$

- Semi-discrete form of PDE (with Euler scheme) at time n :

$$\frac{u^{n+1} - u^n}{\Delta t} + \boxed{u^n u_x^{n+1} - \kappa u_{xx}^{n+1}} = 0 \quad (2)$$

- Enrichment functions inside each element at time step n are the free-space solutions to steady analogs of (2):

$$\mathcal{V}^{E,n} = \text{span}\{u^n(x) : u^{n-1}(\bar{x}_e)u_x^n - \kappa u_{xx}^n = 0, x \in \Omega^e\}$$

where

$\mathcal{V}_e^{E,n}$ = enrichment field inside element Ω^e at time step n

$\bar{x}_e \equiv$ midpoint of element Ω^e



Matrix Problem and Implementation for Unsteady Non-Linear DEM (Pure DGM Element)

- Element-level semi-discrete matrix problem:

$$\begin{pmatrix} \mathbf{m}^{EE} & \mathbf{0} \\ \mathbf{0} & \mathbf{0} \end{pmatrix} \begin{pmatrix} \dot{\mathbf{u}}^E \\ \dot{\boldsymbol{\lambda}}^h \end{pmatrix} + \begin{pmatrix} \mathbf{k}^{EE}(\mathbf{u}^E) & \mathbf{k}^{EC} \\ \mathbf{k}^{CE} & \mathbf{0} \end{pmatrix} \begin{pmatrix} \mathbf{u}^E \\ \boldsymbol{\lambda}^h \end{pmatrix} = \begin{pmatrix} \mathbf{0} \\ \mathbf{0} \end{pmatrix}$$

- Apply time-integration scheme to obtain fully-discrete, element-level problem:

$$\begin{pmatrix} \mathbf{m}^{EE} + \Delta t \mathbf{k}^{EE}(\mathbf{u}^{E,n}) & \Delta t \mathbf{k}^{EC} \\ \Delta t \mathbf{k}^{CE} & \mathbf{0} \end{pmatrix} \begin{pmatrix} \mathbf{u}^{E,n+1} \\ \boldsymbol{\lambda}^{h,n+1} \end{pmatrix} = \begin{pmatrix} \mathbf{m}^{EE} & \mathbf{0} \\ \mathbf{0} & \mathbf{0} \end{pmatrix} \begin{pmatrix} \mathbf{u}^{E,n} \\ \boldsymbol{\lambda}^{h,n} \end{pmatrix}$$

- Eliminate enrichment dofs $\mathbf{u}^{E,n+1}$ at the element-level by a static condensation:

$$\Delta t \mathbf{k}^{CE} [\mathbf{m}^{EE} + \Delta t \mathbf{k}^{EE}(\mathbf{u}^{E,n})]^{-1} \mathbf{k}^{EC} \boldsymbol{\lambda}^{h,n+1} = \mathbf{k}^{CE} [\mathbf{m}^{EE} + \Delta t \mathbf{k}^{EE}(\mathbf{u}^{E,n})]^{-1} \mathbf{m}^{EE} \mathbf{u}^{E,n}$$



A Non-Linear BVP with a Weak Shock

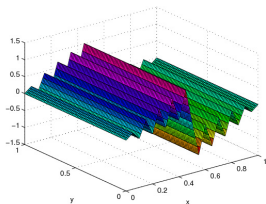
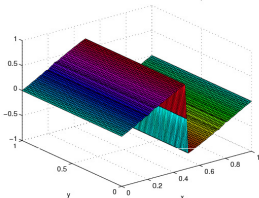
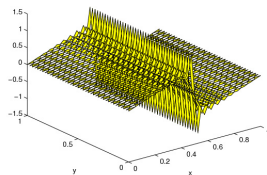
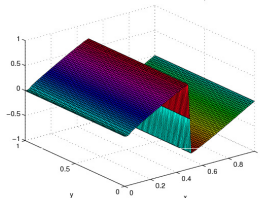
$$\begin{cases} u_t + uu_x - \kappa u_{xx} = 0, & \text{in } \Omega \equiv (0, 1) \\ u(0, t) = u(1, t) = 0 \\ u(x, 0) = \sin(2\pi x), & \text{in } \Omega \equiv (0, 1) \end{cases} \quad (3)$$

- Can show using method of characteristics that solution to (3) exhibits a weak shock at the point $x_s \equiv 0.5$ at time $T_s \equiv \frac{1}{2\pi}$ in the limit as $\kappa \rightarrow 0$ ($Pe \rightarrow \infty$).
- Standard finite elements run into trouble in the vicinity of the shock: produce central-difference type spurious, non-physical oscillations (next slide).
- DGM/DEM elements to be tested:

Element	Enrichment Functions
$Q - 3 - 1$	$u_1^{E,n} = e^{u^{n-1}(\bar{x}_e)(x-x_r^e)}, u_2^{E,n} = 1, u_3^{E,n} = \sin(2\pi x)$
$Q - 2 - 1^+$	$u_1^{E,n} = e^{u^{n-1}(\bar{x}_e)(x-x_r^e)}, u_2^{E,n} = x^2$



Preliminary Numerical Results ($\kappa = 10^{-3}$, $T = 0.5$, $\Delta t = 0.05$, 20×20 uniform mesh)

 Q_1  $Q - 3 - 1$  Q_2  $Q - 2 - 1^+$

Very promising: DEM solutions are oscillation free!

